

# Permeabilization via the P2X<sub>7</sub> Purinoreceptor Reveals the Presence of a Ca<sup>2+</sup>-activated Cl<sup>−</sup> Conductance in the Apical Membrane of Murine Tracheal Epithelial Cells\*

Received for publication, June 7, 2000, and in revised form, August 8, 2000  
Published, JBC Papers in Press, August 15, 2000, DOI 10.1074/jbc.M004953200

Sherif E. Gabriel‡§, Mariya Makhlin‡, Elena Martsen‡, Emma J. Thomas¶, Mike I. Lethem¶, and Richard C. Boucher‡

From the ‡Cystic Fibrosis/Pulmonary Research and Clinical Treatment Center, University of North Carolina, Chapel Hill, North Carolina 27599 and the ¶School of Pharmacy and Biomolecular Sciences, University of Brighton, Brighton BN2 4GJ, United Kingdom

Calcium-activated Cl<sup>−</sup> secretion is an important modulator of regulated ion transport in murine airway epithelium and is mediated by an unidentified Ca<sup>2+</sup>-stimulated Cl<sup>−</sup> channel. We have transfected immortalized murine tracheal epithelial cells with the cDNA encoding the permeabilizing P2X<sub>7</sub> purinoreceptor (P2X<sub>7</sub>-R) to selectively permeabilize the basolateral membrane and thereby isolate the apical membrane Ca<sup>2+</sup>-activated Cl<sup>−</sup> current. In P2X<sub>7</sub>-R-permeabilized cells, we have demonstrated that UTP stimulates a Cl<sup>−</sup> current across the apical membrane of CF and normal murine tracheal epithelial cells. The magnitude of the UTP-stimulated current was significantly greater in CF than in normal cells. Ion substitution studies demonstrated that the current exhibited a permselectivity sequence of Cl<sup>−</sup> > I<sup>−</sup> > Br<sup>−</sup> > gluconate<sup>−</sup>. We have also determined a rank order of potency for putative Cl<sup>−</sup> channel blockers: niflumic acid ≥ 5-nitro-2-(3-phenylpropylamino)benzoic acid > 4,4'-diisothiocyanostilbene-2,2'-disulfonate > glybenclamide >> diphenylamine-2-carboxylate, tamoxifen, and *p*-tetra-sulfonato-tetra-methoxy-calix[4]arene. Complete characterization of this current and the corresponding single channel properties could lead to the development of a new therapy to correct the defective airway surface liquid in cystic fibrosis patients.

Chloride secretion across the airway epithelium can be stimulated by a number of secretagogues that activate distinct second messenger transduction mechanisms (reviewed in Refs. 1 and 2). The cystic fibrosis (CF)<sup>1</sup> gene product, the cystic fibrosis transmembrane conductance regulator (CFTR), accounts for the cAMP-regulated apical Cl<sup>−</sup> conductance (3, 4). There is, however, compelling evidence that a separate Ca<sup>2+</sup>-

activated apical Cl<sup>−</sup> conductance (CaCC) exists. A large class of ligands, including histamine (5, 6), bradykinin (7, 8), and extracellular ATP (9–11), has been shown to activate CaCC across the apical membrane of airway epithelia. The unique identity of this pathway in airway epithelia was established in studies of CF nasal epithelia, which demonstrated that Ca<sup>2+</sup> ionophores are effective Cl<sup>−</sup> secretagogues in CF tissues (12–14). Moreover, in the airways of the CFTR(−/−) knockout mouse, which definitively lacks CFTR (15), not only is the CaCC pathway preserved, but it appears to be up-regulated (16).

In the airway epithelium, Cl<sup>−</sup> secretion is dependent on the development of a favorable driving force, because at basal conditions Cl<sup>−</sup> is at or near electrochemical equilibrium across the apical membrane. Ca<sup>2+</sup><sub>i</sub> can stimulate Cl<sup>−</sup> secretion by multiple mechanisms. Elevation of Ca<sup>2+</sup><sub>i</sub> can directly activate an apical membrane-localized Cl<sup>−</sup> conductance and thereby stimulate an apical exit pathway for Cl<sup>−</sup> secretion. Ca<sup>2+</sup> mobilizing agents can also cause a hyperpolarization in the cell to generate a driving force for Cl<sup>−</sup> secretion across the apical membrane by either (or both) inhibiting an apical membrane Na<sup>+</sup> conductance (17) or activating a basolateral K<sup>+</sup> conductance. Thus study of Ca<sup>2+</sup><sub>i</sub>-activated Cl<sup>−</sup> conductance in the apical membrane of a polarized epithelium requires a means to identify the contributions of apical Cl<sup>−</sup> conductance in isolation from other actions.

Previous studies in non-polarized secretory epithelia, *e.g.* airway epithelia or T<sub>84</sub> cells plated as isolated or dissociated cells, have shown outwardly rectifying Cl<sup>−</sup> currents stimulated by intracellular Ca<sup>2+</sup> and sensitive to 4,4'-diisothiocyanostilbene-2,2'-disulfonate (DIDS) (18–24). These descriptions have included such a wide range of Cl<sup>−</sup> channel characteristics that no consensus on the characteristics of this channel can be achieved (25–28). Recently, a family of putative CaCC genes has been cloned (29–32). The single channel properties and the cellular localization of these gene products, however, have not yet been determined. Thus, no indisputably apical Ca<sup>2+</sup>-activated Cl<sup>−</sup> channel has been identified at either the molecular or single channel level.

We have recently identified a CaCC current expressed in immortalized CF and normal murine tracheal epithelial cell lines (33). In the current study we used permeabilization of the basolateral membrane to determine the basic biophysical properties of the CaCC current in a functionally isolated apical membrane of airway epithelial cells. We have accomplished basolateral permeabilization by a novel approach involving stable transfection of the P2X<sub>7</sub> purinoreceptor (P2X<sub>7</sub>-R) into our murine CF tracheal epithelial cell line. The P2X<sub>7</sub>-R is

\* This work was supported by Grant 99PO from the Cystic Fibrosis Foundation and Grant HL62564 from the National Institutes of Health (both to S. E. G.). The costs of publication of this article were defrayed in part by the payment of page charges. This article must therefore be hereby marked "advertisement" in accordance with 18 U.S.C. Section 1734 solely to indicate this fact.

§ To whom correspondence should be addressed: CF/PRT Center & Dept. of Pediatrics, University of North Carolina, Chapel Hill, NC 27599. Tel.: 919-966-7058; Fax: 919-966-7524; E-mail: [sgabriel@med.unc.edu](mailto:sgabriel@med.unc.edu)

<sup>1</sup> The abbreviations used are: CF, cystic fibrosis; P2X<sub>7</sub>-R, P2X<sub>7</sub> purinoreceptor; CaCC, Ca<sup>2+</sup>-activated Cl<sup>−</sup> conductance; CFTR, cystic fibrosis transmembrane conductance regulator; KBR, Krebs bicarbonate Ringer solution; NFA, niflumic acid; NPPB, 5-nitro-2-(3-phenylpropylamino)benzoic acid; DIDS, 4,4'-diisothiocyanostilbene-2,2'-disulfonate; DPC, diphenylamine-2-carboxylate; TS-TM calixarene, *p*-tetra-sulfonato-tetra-methoxy-calix[4]arene.

unique within its family, because binding of nucleotides ( $\text{ATP}^{4-}$  is the preferred agonist) to this receptor results in the formation of a membrane pore that is capable of conducting molecules as large as 900 daltons (34, 35). The pore is not ion-selective and allows for free diffusion of both cations and anions. Thus, by application of ATP selectively to the basolateral solution, we can selectively permeabilize this barrier.

We report here the characterization of CaCC in the apical membrane of a CF tracheal epithelial cell line when activated by different classes of  $\text{Ca}^{2+}$ -mobilizing agents (UTP and ionomycin). We have determined the halide selectivity and inhibitor sensitivity of this  $\text{Cl}^-$  current unambiguously localized to the apical membrane. Importantly, these observations will provide us with the hallmark characteristics for comparison with subsequent whole cell and single channel studies and will enable us to evaluate CaCC candidate genes. A greater understanding of the characteristics and mechanism of regulation of the CaCC pathway is essential for development of pharmacological therapies designed to use CaCC as an alternate  $\text{Cl}^-$  channel to replace the defective CFTR.

#### EXPERIMENTAL PROCEDURES

**Cell Culture**—These studies utilized the immortalized murine tracheal epithelial cell line (MTE18) derived from the CFTR(−/−) knockout mouse, described previously (33). Cells were maintained and cultured at 33 °C, the permissive temperature for the immortalizing tsA58 TAg activity (33) on “Transwell-col” culture inserts. Culture medium consisted of a 1:1 mix of Ham’s F12 and 3T3 fibroblast-conditioned medium supplemented with the following hormones: transferrin (2.5 mg/ml), insulin (5 mg/ml), epidermal growth factor (12.5 ng/ml), endothelial cell growth supplement (1.875 mg/ml), triiodothyronine (15 nM), hydrocortisone (0.5 mM), and  $\text{CaCl}_2$  (0.5 mM). Cells were harvested for experimental studies by trypsinization and plated at high density ( $2 \times 10^4$  cells per  $\text{mm}^2$ ) onto tissue culture inserts (collagen matrix supports with a 4.5-mm plating diameter) and evaluated for confluence by daily monitoring of transepithelial resistance ( $R_T$ ) and potential difference ( $V_T$ ). Only monolayers generating at least a 1.0-millivolt (mV)  $V_T$  and a  $100\text{-}\Omega\text{-cm}^2$  resistance (after the resistance of the permeable support is subtracted) were used for Ussing chambers studies, typically 5–7 days after plating.

**Ussing Chamber Studies**—Electrical measurements, *i.e.*  $V_T$ ,  $R_T$ , and short-circuit current ( $I_{SC}$ ), were made on cell monolayers mounted in Ussing chambers. Monolayers were bathed in a Krebs bicarbonate Ringer solution (KBR) on both the luminal and the serosal sides. Serosal  $\text{Ca}^{2+}$  was buffered to 300 nM with the addition of EGTA (achieved by the addition of 1 mM EGTA and 0.925 mM  $\text{Ca}^{2+}$ ). Other alterations to the bathing solutions are listed in the figure legends. All bathing solutions were bubbled with 95%  $\text{O}_2$ , 5%  $\text{CO}_2$  and maintained at 37 °C.  $V_T$  was clamped to zero and pulsed to  $\pm 10$  mV for a 0.5-s duration every minute. Electrometer output was digitized online and  $I_{SC}$ ,  $R_T$ , and calculated transepithelial potential ( $V_T$ ) were displayed on a video monitor and stored on a computer hard drive. Drugs were added from concentrated stock solutions to either luminal and/or serosal sides of the tissue. To eliminate the contribution of apical  $\text{Na}^+$  channels, amiloride ( $10^{-4}$  M) was added to the luminal bath at the outset of all experiments. Data are expressed as mean  $\pm$  S.E. for the number of experiments ( $n$ ). Student’s *t* test was used to determine statistical significance between means.

**Permeabilization**—Basolateral membrane permeabilization was achieved by stable transfection of the recombinant P2X<sub>7</sub>-R (a generous gift from Dr. George Dubyak) into the MTE18 cell line. A cDNA construct of the P2X<sub>7</sub>-R was cloned into a retroviral expression vector with a selectable puromycin-resistance gene. Infection of the MTE18 cell line with this retroviral vector and selection of resistant colonies in puromycin-containing media resulted in the identification of several cell clones that were puromycin-resistant and were verified for expression of P2X<sub>7</sub>-R. These P2X<sub>7</sub>-R-expressing cells were plated on membrane supports and used for Ussing chamber studies.

Following recording of stable baseline  $I_{SC}$  and  $R_T$  (15–20 min in symmetrical  $\text{Cl}^-$  KBR solutions), 1 mM  $\text{ATP}^{4-}$  (UTP is not an agonist for the P2X<sub>7</sub>-R) was added to the serosal solution and serosal  $\text{Mg}^{2+}$  was reduced to 100  $\mu\text{M}$  to activate the pore (divalent cations inhibit pore formation). Following successful permeabilization, documented by a drop in the  $I_{SC}$  to 0  $\mu\text{A}/\text{cm}^2$ , the luminal solution was diluted by three

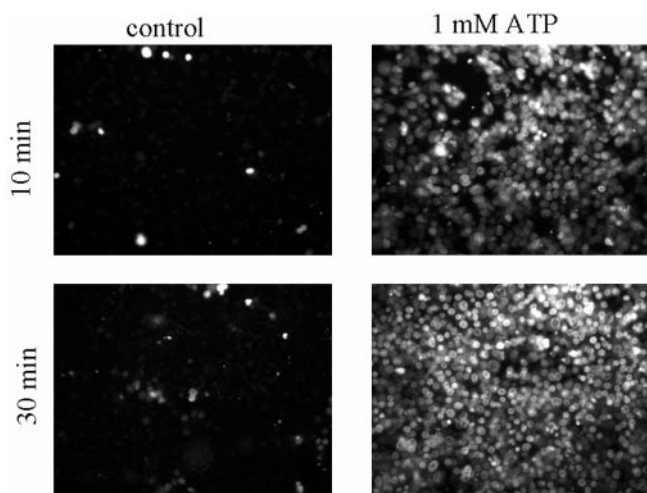


**FIG. 1. ATP-mediated permeabilization of the basolateral membrane of P2X<sub>7</sub>-R monolayers.** P2X<sub>7</sub>-R-expressing cells were exposed to 10  $\mu\text{M}$  ToPro-1-iodide in the absence (left two panels) or presence (right two panels) of 1 mM ATP for 10 or 30 min. Cells were photographed on a fluorescence inverted microscope with identical exposure times.

successive 1-ml replacements of KBR with a low  $\text{Cl}^-$  containing (4.8 mM  $\text{Cl}^-$ , 110 mM gluconate $^-$ ) KBR. This maneuver generates a gradient for  $\text{Cl}^-$  secretion with a serosal  $\text{Cl}^-$  concentration of 115 mM and a final luminal  $\text{Cl}^-$  concentration of  $\approx 68$  mM.  $\text{Ca}^{2+}$ -mobilizing agents were added to the luminal solution after the final dilution step. Anion selectivity was determined by a similar strategy used to generate the  $\text{Cl}^-$  gradients. Briefly, three successive 1-ml replacements of the luminal solution with a modified KBR solution containing a halide ion ( $\text{I}^-$ ,  $\text{Br}^-$ ) were substituted for  $\text{Cl}^-$  (*e.g.* 4.8 mM  $\text{Cl}^-$ , 110 mM  $\text{I}^-$ ). The inhibitor profile of CaCC was determined by the addition of inhibitors to the luminal solution after the imposition of the  $\text{Cl}^-$  gradient and prior to stimulation by UTP. All experiments consisted of alterations in the ion composition of the mucosal or serosal solution, followed by CaCC activation by addition of luminal UTP.

In a subset of experiments we used the  $\alpha$ -toxin of *Staphylococcus aureus* to permeabilize MTE18 or MTE7b (CFTR(+/-) cells) monolayers not expressing the P2X<sub>7</sub>-R. 1000 units of  $\alpha$ -toxin was introduced to the serosal compartment bathing MTE18 or MTE7b monolayers and monitored for  $\sim 60$  min until the  $I_{SC}$  dropped to 0  $\mu\text{A}/\text{cm}^2$ , indicating permeabilization. Subsequent dilutions and agonist additions were performed as described for P2X<sub>7</sub>-R monolayers.

**Data Analysis**—In CF and normal airway epithelial cells, mucosal nucleotides, ATP or UTP, acting via purinergic receptors cause an increase in  $I_{SC}$  by reducing the apical membrane resistance with little or no effect on the basolateral or shunt resistance, *i.e.* by directly activating an apical membrane conductance (11). All experiments were performed under voltage clamp conditions (clamped to 0 mV) and in the presence of a  $\text{Cl}^-$  gradient followed by the addition of mucosal UTP. Our experimental protocol defines the CaCC current as  $\Delta I_{CaCC} = I_{UTP} - I_{gradient}$ . Because the transepithelial potential is clamped to 0 mV, the equilibrium potential for  $\text{Cl}^-$  can be calculated as  $E_{Cl^-} = \Delta I_{CaCC} \Delta G_{CaCC}$  and is determined by the chemical driving force imposed as a result of the  $\text{Cl}^-$  gradient. This measured  $E_{Cl^-}$  should ideally equal the calculated  $E_{Cl^-}$  determined by the Nernst equation. We used the measured  $E_{ion}$  ( $\text{Cl}^-$ ,  $\text{Br}^-$ ,  $\text{I}^-$ ) values to determine a permeability sequence. Apparent differences between the measured  $E_{ion}$  and Nernst equation-calculated  $E_{ion}$  values are likely caused by ion permeation and accumulation in the unstirred layer closely adjacent to the membrane surface (37).

**Materials**—All biochemicals used were obtained from commercial sources and were of tissue culture grade or better.

#### RESULTS

Transfection and expression of P2X<sub>7</sub>-R in MTE18 cells followed by incubation of monolayers with 1 mM ATP and 10  $\mu\text{M}$  ToPro-1-iodide (a membrane-impermeant dye that fluoresces when bound to DNA,  $M_r = 645$ ) demonstrates efficient membrane permeabilization (Fig. 1). Although cells exposed to ATP for either 10 or 30 min showed distinct intracellular fluores-

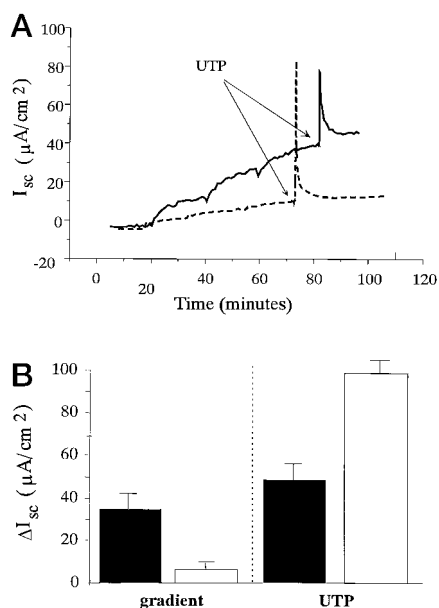


**FIG. 2. Characteristic CaCC current response in P2X<sub>7</sub>-R permeabilized MTE18 monolayers.** A, typical  $I_{sc}$  responses in P2X<sub>7</sub>-R-expressing MTE18 monolayers permeabilized by 1-mM serosal ATP (solid line) and non-permeabilized MTE18 monolayers (dashed line). Both permeabilized and non-permeabilized monolayers were treated similarly during the rest of the experimental protocol. Luminal  $\text{Cl}^-$  was successively diluted by replacement with a sodium gluconate solution to achieve a final luminal  $\text{Cl}^-$  concentration of 68 mM, and 10  $\mu\text{M}$  UTP was added to the luminal solution (as indicated by the arrows). B, mean  $\text{Cl}^-$  current responses in permeabilized (filled bars) and non-permeabilized (open bars) MTE18 monolayers. Gradient responses (left two bars) represent the total  $I_{sc}$  response following the final solution change. The  $I_{sc}$  in response to UTP (10  $\mu\text{M}$ ) addition following the imposition of the  $\text{Cl}^-$  gradient is shown in the right two bars. Filled bars represent the mean current response of P2X<sub>7</sub>-R monolayers exposed to serosal ATP (permeabilized,  $n = 13$ ), and open bars represent P2X<sub>7</sub>-R monolayers in the absence of serosal ATP (non-permeabilized,  $n = 14$ ). Values represent mean and S.E. for each condition.

cence (Fig. 1, right two panels), P2X<sub>7</sub>-R-expressing cells not exposed to ATP showed no significant fluorescence beyond background levels (Fig. 1, left two panels). Control MTE18 cells or MTE18 cells expressing the control LISN vector, did not show any intracellular fluorescence in response to a 30-min exposure with 1 mM ATP (data not shown). We used this cell line (murine tracheal CFTR(-/-) epithelial cells, expressing P2X<sub>7</sub>-R) and selective permeabilization of the basolateral membrane to characterize CaCC resident in the apical membrane of airway epithelial cells.

Basolateral membrane permeabilization of murine tracheal epithelial cells followed by imposition of a  $\text{Cl}^-$  gradient and activation by mucosal UTP revealed the presence of an apical membrane  $\text{Cl}^-$  current (Fig. 2). Application of a cell to lumen  $\text{Cl}^-$  gradient resulted in a greater response in monolayers exposed to serosal 1 mM ATP than to cells not permeabilized by ATP (Fig. 2B,  $34.4 \pm 9.2$  versus  $7.5 \pm 2.4$   $\mu\text{A}/\text{cm}^2$ ). Importantly, addition of mucosal UTP to permeabilized cell monolayers was still capable of stimulating an increase in  $I_{sc}$  consistent with  $\text{Cl}^-$  secretion (Fig. 2A, solid line trace, and Fig. 2B, right panel, filled bar). Similar responses to both an imposed  $\text{Cl}^-$  gradient and mucosal UTP addition ( $\Delta I_{sc} = 54 \pm 7.4$  and  $32.1 \pm 8.9$   $\mu\text{A}/\text{cm}^2$ ,  $n = 8$ , respectively) were observed in MTE18 (CF) monolayers permeabilized by *S. aureus*  $\alpha$ -toxin. The magnitude of the  $\text{Cl}^-$  secretory response to the purinergic agonist UTP was significantly greater in  $\alpha$ -toxin-permeabilized MTE18 preparations than in  $\alpha$ -toxin-permeabilized MTE7B (normal) preparations ( $32.1 \pm 8.9$   $\mu\text{A}/\text{cm}^2$ ,  $n = 8$ ;  $10.9 \pm 3.7$   $\mu\text{A}/\text{cm}^2$ ,  $n = 8$ , respectively,  $p < .001$ ). Elevation of intracellular  $\text{Ca}^{2+}$  by

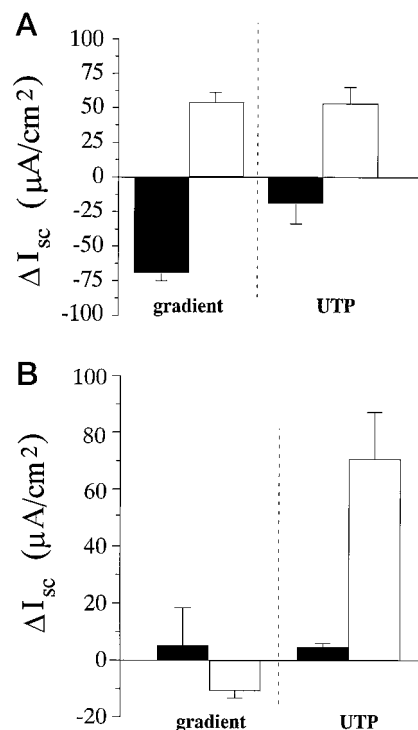


**FIG. 3. Effects of altering the  $\text{Cl}^-$  gradient in P2X<sub>7</sub>-R monolayers.** A, dilution of the serosal  $\text{Cl}^-$  concentration generates a mucosal to serosal  $\text{Cl}^-$  current. All bars represent P2X<sub>7</sub>-R monolayers permeabilized by 1 mM serosal ATP.  $\text{Cl}^-$  gradients were generated as described above (i.e. dilution of either the luminal or serosal solution to achieve a  $\text{Cl}^-$  concentration ratio of 115 mM to 68 mM). Filled bars ( $n = 10$ ) represent monolayers with 115 mM mucosal  $\text{Cl}^-$  and 68 mM serosal  $\text{Cl}^-$  concentrations, and open bars ( $n = 13$ ) represent monolayers with 115 mM serosal  $\text{Cl}^-$  and 68 mM mucosal  $\text{Cl}^-$  concentration. The response to 10  $\mu\text{M}$  luminal UTP following the generation of the  $\text{Cl}^-$  gradient is shown in the right two bars. B,  $\text{Cl}^-$  secretion induced with lower serosal  $\text{Cl}^-$  concentrations. All conditions contain 35 mM  $\text{Cl}^-$  in the serosal solution and a final mucosal  $\text{Cl}^-$  concentration of  $\approx 20$  mM. Filled bars represent the mean current response of P2X<sub>7</sub>-R monolayers exposed to serosal ATP (permeabilized,  $n = 11$ ), and open bars represent P2X<sub>7</sub>-R monolayers in the absence of serosal ATP (non-permeabilized,  $n = 18$ ). The  $I_{sc}$  response to 10  $\mu\text{M}$  luminal UTP is shown in the right two bars. Values represent mean and S.E. for each condition.

inclusion of the ionophore, ionomycin (1  $\mu\text{M}$ ), showed a similar ability to stimulate  $\text{Cl}^-$  secretion in permeabilized CF monolayers ( $25.8 \pm 6.6$   $\mu\text{A}/\text{cm}^2$ ,  $n = 8$ ).

We have used several solution changes to verify that the observed current in MTE18-P2X<sub>7</sub>-R cells is a  $\text{Cl}^-$  current. As shown above (Fig. 2)  $\text{Cl}^-$  secretion (serosal to mucosal) is stimulated by imposition of a chemical gradient (i.e. lower  $\text{Cl}^-$  concentration in the luminal solution). Reversal of this gradient, by decreasing the serosal  $\text{Cl}^-$  concentration in permeabilized preparations, results in stimulation of " $\text{Cl}^-$  absorption" (mucosal to serosal) (Fig. 3). When the  $\text{Cl}^-$  concentration in the luminal solution was maintained at 115 mM and the serosal solution was sequentially reduced, an absorptive  $\text{Cl}^-$  current was recorded (Fig. 3A). The magnitude of the response was similar to the response observed for  $\text{Cl}^-$  secretion (Fig. 2) but in the opposite direction ( $68.8 \pm 7.4$  versus  $54.1 \pm 8.2$   $\mu\text{A}/\text{cm}^2$ , respectively). Mucosal UTP was likewise able to augment this basal level of  $\text{Cl}^-$  absorption by  $18.2 \pm 15.8$   $\mu\text{A}/\text{cm}^2$ . MTE18-P2X<sub>7</sub>-R cells that were not permeabilized (not exposed to serosal ATP) did not respond to the imposed absorptive gradient (data not shown).

We also studied the magnitude of the  $\text{Cl}^-$  current when the serosal  $\text{Cl}^-$  concentration was reduced to levels that approximate intracellular  $\text{Cl}^-$  ( $\sim 35$  mM). We then imposed an out-



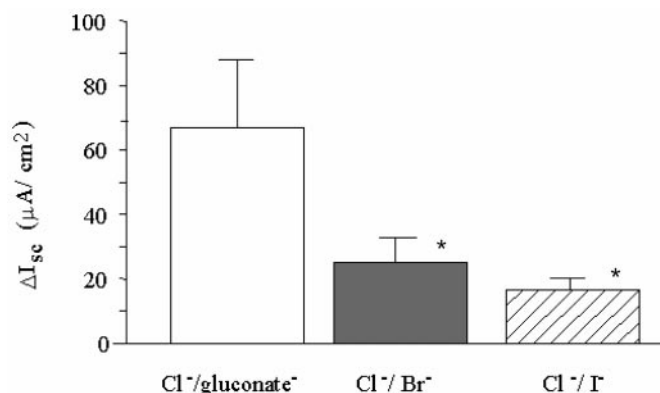


FIG. 4. Halide selectivity sequence in  $\text{P2X}_7\text{-R}$  monolayers. All bars represent  $\text{P2X}_7\text{-R}$  monolayers permeabilized by 1 mM serosal ATP and contain 115 mM serosal  $\text{Cl}^-$ . Mucosal solutions were diluted to achieve a final  $\text{Cl}^-$  concentration of 68 mM with the replacement anion, gluconate (open bars,  $n = 11$ ), bromide (filled bars,  $n = 7$ ), or iodide (hatched bars,  $n = 12$ ). Total luminal anion concentrations were always maintained at 115 mM (e.g. 68 mM  $\text{Cl}^-$  and 47 mM gluconate). Values represent mean  $\pm$  S.E. for each condition. The asterisk represents statistical significance ( $p < 0.01$ ) as determined by the Student's  $t$  test between gluconate and bromide means and gluconate and iodide means.

wardly directed  $\text{Cl}^-$  gradient by reducing luminal  $\text{Cl}^-$  to a similar ratio as previously studied (final mucosal  $\text{Cl}^-$  was diluted to a value of approximately 56% of the serosal concentration). Under these conditions, UTP was still capable of stimulating a characteristically similar  $\text{Cl}^-$  response, although the magnitude of the response was smaller than that observed with higher  $\text{Cl}^-$  concentrations (Fig. 3B).

The previous series of experiments involved dilution of the  $\text{Cl}^-$  concentration by substitution with the less permeant anion gluconate $^-$ . This in effect results in a bi-ionic permselectivity relation, which provides an opportunity to determine the relative permeabilities of  $\text{Cl}^-$  and gluconate. We subsequently performed similar experiments in which  $\text{Cl}^-$  was substituted with  $\text{Br}^-$  or  $\text{I}^-$  (Fig. 4). Substitution of  $\text{Cl}^-$  with gluconate showed an increase in secretory  $\text{Cl}^-$  current (serosal to mucosal) as expected for a  $\text{Cl}^-$  dominated current. Both bromide and iodide substitution significantly attenuated the magnitude of this current, indicating that both of these halides,  $\text{I}^-$  and  $\text{Br}^-$  were more permeable than gluconate but less permeable than  $\text{Cl}^-$ . Simply considering the  $\text{Cl}^-$  concentration on either side of the membrane, the Nernst equation would predict an equilibrium potential of  $-13.6$  mV. With gluconate as the counterion, we calculated an  $E_{\text{Cl}^-}$  of  $\approx -9.8$  mV. When bromide was substituted for  $\text{Cl}^-$ , the calculated  $E_{\text{Cl}^-}$  was  $\approx -6.7$  mV, and when iodide was used as the counterion,  $E_{\text{Cl}^-}$  was calculated to be  $\approx -3.8$  mV. These increasing differences away from the Nernst equilibrium potential describe an anion selectivity sequence that is  $\text{Cl}^- > \text{I}^- > \text{Br}^- > \text{gluconate}^-$ .

Several putative  $\text{Cl}^-$  channel blockers were investigated for inhibition of UTP-stimulated  $\text{Cl}^-$  secretion in  $\text{P2X}_7\text{-R}$ -permeabilized MTE18 cells (Fig. 5). The most efficacious compounds appeared to be niflumic acid (NFA) (100  $\mu\text{M}$ ) and 5'-nitrophenyl-propylbenzoate (NPPB; 100  $\mu\text{M}$ ), both of which inhibited approximately 90% of the  $\text{CaCC}$ -mediated current. The most routinely used  $\text{Cl}^-$  channel blocker, DIDS (100  $\mu\text{M}$ ), inhibited slightly more than 60% of the UTP-stimulated current, whereas glybenclamide (100  $\mu\text{M}$ ), a  $\text{K}^+$  channel blocker that has been shown to have efficacy against CFTR (38), blocked about 40% of the UTP-stimulated current. Finally, TS-TM calixarene (1  $\mu\text{M}$ ), a reported inhibitor specific for the outward rectifying  $\text{Cl}^-$  channel (36), the anti-estrogen tamoxifen (10  $\mu\text{M}$ ), shown to inhibit the human  $\text{ClCA2}$  channel (32), and

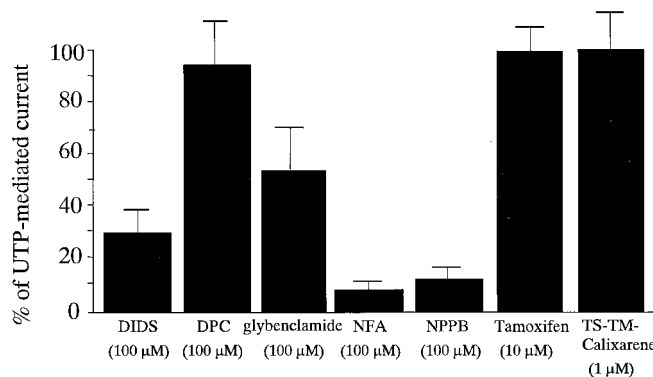


FIG. 5. Inhibitor effects on  $\text{Cl}^-$  currents measured in  $\text{P2X}_7\text{-R}$ -permeabilized monolayers. All monolayers were permeabilized by 1 mM serosal ATP and exposed to the serosal to mucosal  $\text{Cl}^-$  gradient as described above. Inhibitors, DIDS (100  $\mu\text{M}$ ,  $n = 8$ ), DPC (100  $\mu\text{M}$ ,  $n = 8$ ), glybenclamide (100  $\mu\text{M}$ ,  $n = 8$ ), NFA (100  $\mu\text{M}$ ,  $n = 8$ ), NPPB (100  $\mu\text{M}$ ,  $n = 8$ ), tamoxifen (10  $\mu\text{M}$ ,  $n = 8$ ), and TS-TM calixarene (1  $\mu\text{M}$ ,  $n = 9$ ) were added to the mucosal solution prior to addition of 10  $\mu\text{M}$  UTP. Values represent mean  $\pm$  S.E. of percentage inhibition of the UTP response in comparison to permeabilized monolayers treated with vehicle alone prior to UTP.

diphenylamine-2-carboxylate (DPC) (100  $\mu\text{M}$ ) were essentially without effect ( $<10\%$  inhibition) on the UTP-stimulated current.

#### DISCUSSION

We have previously shown that UTP, ionomycin, and thapsigargin are all capable of stimulating a  $\text{Cl}^-$  current in both CF and normal murine airway epithelial cells (33). In that study we demonstrated the presence of the  $\text{Ca}^{2+}$ -activated  $\text{Cl}^-$  current and noted that the magnitude of the current was greater in CF (MTE18) than in normal (MTE7b) cells. In this study we have used permeabilization of the basolateral membrane to focus on an "apically isolated" preparation. Efficacy of permeabilization is apparent by the greater response to the imposed gradient observed in the permeabilized *versus* non-permeabilized preparations (compare filled with open bars in Fig. 2B). Dilutions of the luminal solution in non-permeabilized monolayers leads to only minor changes in current, but subsequent addition of UTP generates a large change in current. In permeabilized preparations, a large increase in current is observed in response to both changes in the  $\text{Cl}^-$  concentration, as well as the addition of UTP. Importantly, nucleotides ATP/UTP acting via the purinoreceptor,  $\text{P2Y}_2$ , have been shown to directly reduce the apical membrane resistance with no effect on the resistance of the tight junction (11). In our experimental design, imposition of a chemical gradient for  $\text{Cl}^-$  is likely to have effects on both the apical membrane conductance and the paracellular pathway, but application of UTP will only stimulate  $\text{Cl}^-$  secretion by activation of an apical membrane  $\text{Cl}^-$  channel. Thus, the response to UTP following permeabilization and imposition of the  $\text{Cl}^-$  gradient is convincing evidence for the existence of a  $\text{Ca}^{2+}$ -activated apical membrane  $\text{Cl}^-$  channel. Furthermore, an increase in  $I_{\text{SC}}$  in response to ionomycin is also confirmatory evidence that the  $\text{Ca}^{2+}$ -mediated effects are the result of an apical  $\text{Cl}^-$  conductance rather than an effect on the paracellular pathway.

In an intact preparation,  $\text{Ca}^{2+}$  activation of  $\text{K}^+$  channels in the basolateral membrane likely plays an important role in maintaining the driving force necessary for  $\text{Cl}^-$  secretion. One obvious advantage of a permeabilized preparation is that we can eliminate the need for basolateral  $\text{K}^+$  channels by imposing a gradient by solution changes and thereby directly focus on the apical membrane. With these maneuvers we have shown that a  $\text{Ca}^{2+}$ -activated  $\text{Cl}^-$  conductance is present in the apical

membrane of murine tracheal epithelial cells. Interestingly, UTP and ionomycin regulate this apical membrane  $\text{Cl}^-$  conductance even when  $\text{Ca}^{2+}_i$  is buffered to moderate levels (300 nM) by EGTA. This suggests that the accessory proteins necessary for regulation are not dialyzed by permeabilization and that the mechanisms for intracellular  $\text{Ca}^{2+}$  release are also well preserved. Somewhat surprising, however, was the observation that UTP consistently activated this  $\text{Cl}^-$  conductance in the presence of 1 mM EGTA. EGTA is relatively slow in terms of buffering  $\text{Ca}^{2+}$  and may not be able to rapidly chelate release from local  $\text{Ca}^{2+}$  stores efficiently (39, 40). This experimental protocol allows us to buffer  $\text{Ca}^{2+}$  to physiological levels and preserves the ability to observe a UTP-mediated current response. These data are consistent with whole cell patch clamp studies that showed ATP-activated  $\text{Cl}^-$  currents in human airway epithelial cells in the presence of 10 mM EGTA (41). We have previously shown that UTP-stimulated currents in non-permeabilized MTE18 cells can be abolished by BAPTA-AM (33). Together, these results suggest that the UTP-stimulated current is  $\text{Ca}^{2+}$ -dependent, but that released  $\text{Ca}^{2+}$  is capable of activating a target before it can be chelated by EGTA.

Heterologous expression of  $\text{P2X}_7$ -R in MTE18 cells provides a reliable, consistent, and rapid technique to generate an apically isolated preparation. Characteristically, the  $\text{Cl}^-$  secretory response to the imposed  $\text{Cl}^-$  gradient and to the luminal addition of UTP is similar to the responses observed in  $\alpha$ -toxin permeabilized monolayers. Challenging  $\text{P2X}_7$ -R-expressing monolayers with ATP and the fluorescent DNA-intercalating agent, ToPro-1-iodide, demonstrated that  $\text{P2X}_7$ -R effectively forms a pore sufficient for dialysis of the intracellular ion solution. These studies show that nearly every cell was expressing  $\text{P2X}_7$ -R and that receptor expression alone did not confer an increase in cell conductance, but rather that receptor occupancy by ATP was an absolute requirement for pore formation. Reversal of the  $\text{Cl}^-$  gradient confirmed that the preparation was permeabilized and also established that the current was  $\text{Cl}^-$ -selective. Stable expression of  $\text{P2X}_7$ -R allows us an opportunity to determine the characteristics of the  $\text{Ca}^{2+}_i$ -activated  $\text{Cl}^-$  conductance of the apical membrane in CF murine tracheal epithelial cells. This novel protocol for membrane permeabilization (transfection and activation of  $\text{P2X}_7$ -R) has the further advantage of serving as a self-contained control for permeabilization. By not exposing the cells to millimolar basolateral ATP, the cells function as an intact monolayer, thus the same monolayer preparation can be used for both non-permeabilized and permeabilized protocols.

We have characterized apical membrane CaCC in these preparations in terms of ion selectivity and inhibitor sensitivity. As mentioned earlier, several reports have provided differing characteristics for the CaCC. We believe that characterization in the CF murine airway apical membrane will provide the hallmark characteristics for this channel for subsequent whole cell and single channel analyses. Initial studies in  $\text{P2X}_7$ -R-permeabilized monolayers (Figs. 2 and 3) demonstrated a  $\text{Cl}^-$  current in response to a gradient that was generated by partial replacement of the mucosal  $\text{Cl}^-$  with the less permeant anion, gluconate. Although this fundamentally important experiment demonstrates the presence of the apical membrane  $\text{Cl}^-$  conductance, it also in fact serves as the first in a series of ion replacement studies. Although gluconate is often used as an "impermeant" anion, it is really only less permeant than the halide series. Therefore, a bi-ionic solution of  $\text{Cl}^-$  and gluconate can be evaluated for permselectivity based on the magnitude of the current response and a calculated equilibrium potential. As observed in Fig. 4, not surprisingly,  $\text{Cl}^-$  is more permeant than gluconate and results in a  $\text{Cl}^-$  current from serosal to mucosal

solution. In contrast, when the mucosal  $\text{Cl}^-$  is partially replaced with iodide or bromide, we observed a smaller UTP-induced secretion and a greater shift from the ideal equilibrium potential, suggesting an ion series for this apical  $\text{Cl}^-$  conductance of  $\text{Cl}^- > \text{I}^- > \text{Br}^- > \text{gluconate}^-$ . This anion selectivity sequence is somewhat similar to other reports of  $\text{Ca}^{2+}$ -activated  $\text{Cl}^-$  channels (14, 41–43) but importantly differs from the selectivity sequence for CFTR (3, 4, 14, 42) or from the CLC superfamily of  $\text{Cl}^-$  channels (44).

$\text{Cl}^-$  channel blockers were investigated to determine a "sensitivity sequence" for the CaCC channel. Pretreatment of permeabilized monolayers with the  $\text{Cl}^-$  channel blockers was used to determine a percentage inhibition of the UTP-mediated  $\text{Cl}^-$  current. The rank order of potency for channel inhibitors appears to be NFA, NPPB ( $\approx 90\%$ ) > DIDS ( $\approx 60\%$ ) > glybenclamide ( $\approx 40\%$ ) >> tamoxifen, TS-TM calixarene, and DPC (0–10%). The very low, nearly non-existent effect of TS-TM calixarene was consistent with previous studies that defined this compound as a specific inhibitor of the outward rectifying  $\text{Cl}^-$  channel (36). The moderate effect of glybenclamide on CaCC was a bit surprising, because this sulfonylurea compound was thought to be fairly specific for K-ATP and CFTR channels (45, 46). In many studies DIDS is reported to be a highly effective inhibitor of  $\text{Ca}^{2+}$ -activated  $\text{Cl}^-$  conductance (18–20, 41, 47), and although we observed moderate inhibition, it was not as effective as NFA. Higher doses of DIDS may generate higher levels of inhibition, but we are sensitive to the concerns of cross-linking that are associated with this compound. In our studies NFA was the most potent inhibitor of CaCC but like many  $\text{Cl}^-$  channel blockers lacks specificity, as it has been shown to also inhibit CFTR in human airways (47, 48). These studies serve to confirm the notion that  $\text{Cl}^-$  channel blockers are notoriously nonspecific, and inhibitor studies should be used simply as another characteristic to define the observed current. That is, an inhibitor order of potency or sensitivity sequence should serve an analogous function as a halide permselectivity sequence. The identity of the current should be defined by a combination of those characteristic sequences rather than any single effect.

Tamoxifen has recently been shown to have inhibitory effects against the human CICA2 channel (32). Interestingly, tamoxifen was without effect in our CF murine tracheal epithelial cells. Furthermore, we have not been able to detect the murine homologue of this channel, mCICA1, by Northern blot analysis in our CF murine tracheal epithelial cells, suggesting that the apical membrane  $\text{Ca}^{2+}_i$ -activated  $\text{Cl}^-$  conductance is mediated by a thus far unidentified gene or protein.

We propose to utilize the activation, inhibition, and selectivity characteristics determined in this study for future experiments studying whole cell currents and single channel properties and ensure that the channel characteristics are consistent at each level of investigation. This systematic approach will result in the unambiguous identification of the murine airway CaCC localized to the apical membrane. Identification of CaCC along with a determination of regional distribution within the lung will permit us to develop strategies to activate CaCC and stimulate  $\text{Cl}^-$  and fluid secretion and thereby ameliorate the dehydration that is foremost in the pathology of cystic fibrosis.

**Acknowledgments**—We thank Drs. J. Stutts and B. Grubb (University of North Carolina) for excellent advice, discussion, and review of this manuscript. We are especially grateful to Dr. George Dubyak (Case Western Reserve) for his kind gift of the cDNA for the  $\text{P2X}_7$ -R. We also thank Dr. John Olsen (University of North Carolina) for assistance with retroviral expression of the  $\text{P2X}_7$ -R. Thanks also to Drs. B. Bridges and A. Singh (University of Pittsburgh) for the generous gift of TS-TM calixarene.

## REFERENCES

1. Boucher, R. C. (1994) *Am. J. Respir. Crit. Care Med.* **150**, 581–593
2. Boucher, R. C. (1994) *Am. J. Respir. Crit. Care Med.* **150**, 271–281
3. Kartner, N., Hanrahan, J. W., Jensen, T. J., Naismith, A. L., Sun, S., Ackerley, C. A., Reyes, E. F., Tsui, L. C., Rommens, J. M., Bear, C. E., and Riordan, J. R. (1991) *Cell* **64**, 681–691
4. Bear, C. E., Li, C., Kartner, N., Bridges, R. J., Jensen, T. J., Ramjeesingh, M., and Riordan, J. R. (1992) *Cell* **68**, 809–818
5. Clarke, L. L., Paradiso, A. M., and Boucher, R. C. (1992) *Am. J. Physiol.* **263**, C1190–C1199
6. Noah, T. L., Paradiso, A. M., Madden, M. C., McKinnon, K. P., and Devlin, T. B. (1991) *Am. J. Respir. Cell Mol. Biol.* **5**, 484–492
7. Clarke, L. L., Paradiso, A. M., Mason, S. J., and Boucher, R. C. (1992) *Am. J. Physiol.* **262**, C644–C655
8. Paradiso, A. M., Cheng, E. H. C., and Boucher, R. C. (1991) *Am. J. Physiol.* **261**, L63–L69
9. Mason, S. J., Paradiso, A. M., and Boucher, R. C. (1991) *Br. J. Pharmacol.* **103**, 1649–1656
10. Knowles, M. R., Clarke, L. L., and Boucher, R. C. (1991) *N. Engl. J. Med.* **325**, 533–538
11. Clarke, L. L., and Boucher, R. C. (1992) *Am. J. Physiol.* **263**, C348–C356
12. Willumsen, N. J., and Boucher, R. C. (1989) *Am. J. Physiol.* **256**, C226–C233
13. Boucher, R. C., Cheng, E. H. C., Paradiso, A. M., Stutts, M. J., Knowles, M. R., and Earp, H. S. (1989) *J. Clin. Invest.* **84**, 1424–1431
14. Anderson, M. P., and Welsh, M. J. (1991) *Proc. Natl. Acad. Sci. U. S. A.* **88**, 6003–6007
15. Snouwaert, J. N., Brigman, K. K., Latour, A. M., Malouf, N. N., Boucher, R. C., Smithies, O., and Koller, B. H. (1992) *Science* **257**, 1083–1088
16. Grubb, B. R., Vick, R. N., and Boucher, R. C. (1994) *Am. J. Physiol.* **266**, C1478–C1483
17. Devor, D. C., and Pilewski, J. M. (199) *Am. J. Physiol.* **276**, C827–C837
18. Egan, M., Flotte, T., Afione, S., Solow, R., Zeitlin, P. L., Carter, B. J., and Guggino, W. B. (1992) *Nature* **358**, 581–584
19. Hanrahan, J. W., and Tabcharani, J. A. (1989) *Ann. N. Y. Acad. Sci.* **574**, 30–43
20. Tabcharani, J. A., and Hanrahan, J. W. (1991) *Am. J. Physiol.* **261**, G992–G999
21. Hanrahan, J. W., and Tabcharani, J. A. (1990) *J. Membr. Biol.* **116**, 65–77
22. Tabcharani, J. A., Jensen, T. J., Riordan, J. R., and Hanrahan, J. W. (1989) *J. Membr. Biol.* **112**, 109–122
23. McCann, J. D., Li, M., and Welsh, M. J. (1989) *J. Gen. Physiol.* **94**, 1015–1036
24. McCann, J. D., Bhalla, R. C., and Welsh, M. J. (1989) *Am. J. Physiol.* **257**, L116–L124
25. Ishikawa, T., and Cook, D. I. (1993) *J. Membr. Biol.* **135**, 261–271
26. Duszyk, M., and Man, S. F. P. (1992) *Biophys. J.* **61**, 583–587
27. Morris, A. P., and Frizzell, R. A. (1993) *Am. J. Physiol.* **264**, C968–C976
28. Kunzelmann, K., Kubitz, R., Grolik, M., Warth, R., and Greger, R. (1992) *Pfluegers Arch.* **421**, 238–246
29. Gruber, A. D., Elble, R. C., Ji, H. L., Schreur, K. D., Fuller, C. M., and Pauli, B. U. (1998) *Genomics* **54**, 200–214
30. Gandhi, R., Elble, R. C., Gruber, A. D., Schreur, K. D., Ji, H. L., Fuller, C. M., and Pauli, B. U. (1998) *J. Biol. Chem.* **273**, 32096–32101
31. Romio, L., Musante, L., Cinti, R., Seri, M., Moran, O., Zegarra-Moran, O., and Galiotta, L. J. V. (1999) *Gene* **228**, 181–188
32. Gruber, A. D., Schreur, K. D., Ji, H. L., Fuller, C. M., and Pauli, B. U. (1999) *Am. J. Physiol.* **276**, C1261–C1270
33. Gabriel, S. E., Thomas, E. J., Makhilina, M., Hardy, S. P., and Lethem, M. I. (1999) *Am. J. Physiol.*, in press
34. Humphreys, B. D., Virginio, C., Surprenant, A., Rice, J., and Dubyak, G. R. (1998) *Mol. Pharmacol.* **54**, 22–32
35. Rassendren, F., Buell, G. N., Virginio, C., Collo G., North A., and Surprenant A. (1997) *J. Biol. Chem.* **272**, 5482–5486
36. Singh, A. K., Venglarik, C. J., and Bridges, R. J. (1995) *Kidney Int.* **48**, 985–993
37. Illek, B., Tam, A. W., Fischer, H., and Machen, T. E. (1999) *Pfluegers Arch.* **437**, 812–822
38. Sheppard, D. N., and Robinson, K. A. (1997) *J. Physiol. (Lond.)* **503**, 333–346
39. Adler, E. M., Augustine, G. J., Duffy, S. N., and Charlton, M. P. (1991) *J. Neurosci.* **11**, 1496–1507
40. Nichols, R. A., and Suplick, G. R. (1996) *Neurosci. Lett.* **211**, 135–137
41. Stutts, M. J., Fitz, J. G., Paradiso, A. M., and Boucher, R. C. (1994) *Am. J. Physiol.* **267**, C1442–C1451
42. Cliff, W. H., and Frizzell, R. A. (1990) *Proc. Natl. Acad. Sci. U. S. A.* **87**, 4956–4960
43. Hwang, T. H., Schwiebert, E. M., and Guggino, W. B. (1996) *Am. J. Physiol.* **270**, C1611–C1623
44. Lorenz, C., Pusch, M., and Jentsch, T. J. (1996) *Proc. Natl. Acad. Sci. U. S. A.* **93**, 13362–13366
45. Sheppard, D. N., and Welsh, M. J. (1992) *J. Gen. Physiol.* **100**, 573–591
46. Schultz, B. D., DeRoos, A. D. G., Venglarik, C. J., Singh, A. K., Frizzell, R. A., and Bridges, R. J. (1996) *Am. J. Physiol.* **271**, L192–L200
47. Gabriel, S. E., Boucher, R. C., and Stutts, M. J. (1993) *Pediatr. Pulmonol.* **9(Suppl.)**, 223–224
48. Zegarra-Moran, O., Sacco, O., Romano, L., Rossi, G. A., and Galiotta, L. J. V. (1997) *J. Membr. Biol.* **156**, 297–305